Mean-field theory for ferroelectricity in Ca$_3$CoMnO$_6$

Y. J. Guo,[1] Shuai Dong,[1,2,3] K. F. Wang,[1] and J.-M. Liu[1,4,*]

[1]*National laboratory of Solid State Microstructures, Nanjing University, Nanjing 210093, China*
[2]*Department of Physics and Astronomy, University of Tennessee, Knoxville, Tennessee 37996, USA*
[3]*Materials Science and Technology Division, Oak Ridge National Laboratory, Tennessee 32831, USA*
[4]*International Center for Materials Physics, Chinese Academy of Sciences, Shenyang, 110016 China*

An elastic Ising model for CoMnO$_6$ chain is proposed to explain the ferroelectricity induced by collinear magnetic order in Ca$_3$CoMnO$_6$, and then a mean-field theory with interchain spin interactions based on this model is developed. With inclusion of the dynamics of polarization domains at finite temperature, we address the rationality of our theory by the good agreement of the calculated electric polarization and dielectric susceptibility with the reported data on Ca$_3$Co$_{2-x}$Mn$_x$O$_6$ ($x \approx 0.96$) [Y. J. Choi, H. T. Yi, S. Lee, Q. Huang, V. Kiryukhin, and S.-W. Cheong, Phys. Rev. Lett. **100**, 047601 (2008)], a typical diatomic Ising spin chain system, while the predicted magnetic susceptibility shows some difference from experiment, the reason of which is discussed.

I. INTRODUCTION

Magnetoelectric (ME) coupling between ferroelectric and magnetic orders, the so-called multiferrocity, has drawn increasing attention recently.[1–4] The microscopic mechanism that causes the multiferrocity has not yet been well approached, although significant progresses have been made in the past few years.[5–9] To describe this coupling between the ferroelectric and magnetic orders for noncollinear and spiral spin-ordered systems, two major microscopic theories have so far been proposed. One is based on the spin current scenario[5,6] and the other deals with the Dzyaloshinskii-Moriya interaction (DMI) (Refs. 10 and 11) which is believed to play the crucial role.[7–9] The two theories illustrate consistently the ferroelectricity identified experimentally for quite a number of spiral spin-ordered systems.

Nevertheless, recent experiments revealed that the spiral spin order is not the prerequisite for the ME coupling and ferroelectricity generation.[12–17] The identification of ferroelectricity in Ca$_3$Co$_{2-x}$Mn$_x$O$_6$ ($x \approx 0.96$) (Refs. 14 and 15) confirmed convincingly that the collinear spin order can generate ferroelectricity too. Ca$_3$CoMnO$_6$ can be viewed as a doped Ca$_3$Co$_2$O$_6$ material where the Co ions are partially replaced by Mn ions. It is well established that the base system, Ca$_3$Co$_2$O$_6$ (CCO), is a model spin-chain compound consisting of parallel one-dimensional Co$_2$O$_6$ infinite chains of face-sharing CoO$_3$ trigonal prisms and octahedral prisms along c axis. Each chain is surrounded by six equally spaced chains, which makes a triangular arrangement on the *ab plane*. The *intrachain* interactions along the c axis are much stronger than the *interchain* ones between the Co$_2$O$_6$ chains.

Similar to CCO, Ca$_3$Co$_{2-x}$Mn$_x$O$_6$ (CCMO) has also much stronger intrachain interactions than the interchain ones and can be structurally viewed as consisting of parallel Ising spin chains with weak interchain interactions. It is a good model for understanding the physics of quasi-one-dimensional spin-chain systems. At $x=1$, in each chain, the Mn and Co ions will occupy the oxygen-octahedron and trigonal-prism sites, respectively, namely, the Mn and Co are alternately arranged

(instead of randomly distributed), which is the key ingredient for the multiferroicity.[16,17] Both the Mn and Co are at the high-spin sites,[16,17] and each Ising chain has an up-up-down-down ($\uparrow\uparrow\downarrow\downarrow$) magnetic order in the ground state.[14–24] Different from spiral magnets, for CCMO the exchange striction from the antiferromagnetic (AFM) interaction between nearest-neighbor (NN) spins along the chain, which shortens the bonds between the antiparallel spins and stretches the bonds between parallel spins, is responsible for the electric polarization. This exchange striction mechanism is relatively simple and can be described by Ising-like model, to be done in this work, while real CCMO has very complicated and delicate multifold interactions and such a relatively simple scenario becomes particularly useful for designing novel multiferroics.

Although quite a few works have been done to illustrate the ferroelectricity in CCMO,[14–17,24] the microscopic mechanism is still confusing, and the results from these works are not fully consistent with each other. Here a tentative approach is necessary to illuminate the confusion from both experimental and theoretical works. In this paper, to explain quantitatively the ferroelectricity induced by exchange striction in CCMO, we start from a CoMnO$_6$ chain, for which an elastic Ising model will be proposed. We first deal with a single diatomic spin chain for the ferroelectricity in the ground state. Then, with inclusion of both the intrachain and interchain interactions of these CoMnO$_6$ chains, a mean-field theory (MFT) is constructed for predicting the electrical and magnetic properties at finite temperature (T). Subsequently, the exciting dynamics of polarization domains is also introduced to account for the deficiency of the MFT due to the broken long-range spin order for this quasi-one-dimensional system at nonzero T.

The rationality of our model is tested by applying it to predict the ferroelectricity in CCMO and related properties as a function of T, respectively, including magnetic and dielectric susceptibilities in comparison with experimental data for CCMO ($x=0.96$). The major objective of this work is to propose a microscopic theory for the ME coupling in Ising spin chain systems.
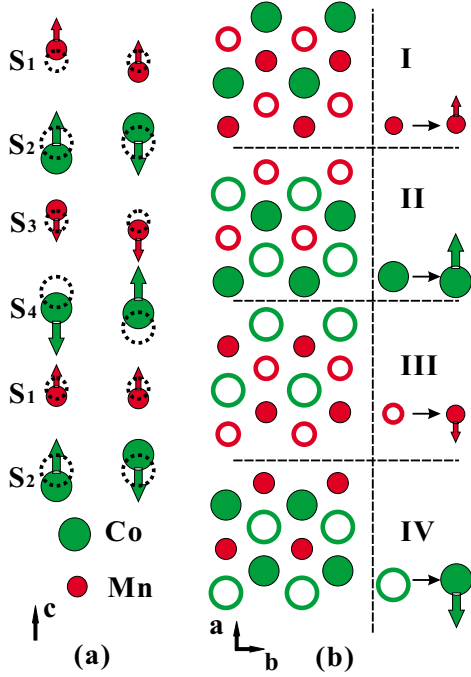
FIG. 1. (Color online) (a) Two configurations of the up-up-down-down Ising chain with alternating Mn (small circle) and Co (big circle) ions. The dashed circle represents the original positions of the ions and the arrows indicate the spin directions. (b) Four consecutive layers of CCMO on the *ab* plane. The real circle represents spin up and open circle represents spin down along the *c* axis.

II. ELASTIC ISING MODEL AND FERROELECTRICITY

We start from the diatomic model for a single Ising spin chain, as the ferroelectricity is induced by the up-up-down-down ($\uparrow\uparrow\downarrow\downarrow$) spin order at $T=0$.[14] At $T=0$, such a spin order can be seen as independent of the interchain interactions which is weak compared to the intrachain interactions. For such a chain with alternating magnetic ions Mn and Co, we consider the NN AFM interaction ($J^a_{\text{Mn-Co}}$) and the next-nearest-neighbor (NNN) AFM interactions ($J^a_{\text{Mn-Mn}}$ and $J^a_{\text{Co-Co}}$) both along the chain direction (*c* axis). In Fig. 1(a) we draw schematically two types of diatomic spin chains aligned along the *c* axis. As expected, the ground state has a $\uparrow\uparrow\downarrow\downarrow$ magnetic order if the strength of these interactions satisfies the conditions $J^a_{\text{Mn-Co}} < J^a_{\text{Mn-Mn}} + J^a_{\text{Co-Co}}$ and $J^a_{\text{Mn-Mn}} > J^a_{\text{Mn-Co}} > J^a_{\text{Co-Co}}$, assuming that the spin moments for ions Mn and Co are equal (their difference is very small).[17] Such Ising chains form a triangular lattice on the *ab* plane, and the configuration is shown in Fig. 1(b) with four consecutive layers. With the consideration of electric-dipole interactions, the Hamiltonian for the Ising model is

$$
\begin{aligned}
H = &- \sum_{\langle ij \rangle} J_{1,i,m} S_{i,m} \cdot S_{j,m} - \sum_{[ij]} J_{2,i,m} S_{i,m} \cdot S_{j,m} - h\mu_B g_l \sum_{i,m} S_{i,m} \\
&- \sum_{\langle mn \rangle} J^e_{\text{AFM}} S_{i,m} \cdot S_{i,n} - \sum_{[mn]} J^e_{\text{FM}} S_{i,m} \cdot S_{i,n} - E \sum_{i,m} P_{i,m} \\
&+ \frac{1}{\varepsilon_c} \sum_{i,m} P^2_{i,m},
\end{aligned}
\tag{1}
$$

where subscript i represents the ith site in a CoMnO$_6$ chain, subscript m represents the mth CoMnO$_6$ chain on the *ab* plane, $\langle ij \rangle$ refers to the NN spin pair and $[ij]$ to the NNN pair along the *c* axis, $J_{1,i}=J^a_{\text{Mn-Co}}$, $J_{2,i}=J^a_{\text{Mn-Mn}}$, or $J^a_{\text{Co-Co}}$ for the interaction between two NNN Mn ions or two NNN Co ions, $S_{i,m}$ represents the spin on site i in the mth CoMnO$_6$ chain, h denotes the magnetic field, μ_B is the Bohr magnon, g_l is the Lande factor, $\langle mn \rangle$ refers to the NN spin pair with an AFM exchange interaction (J^e_{AFM}) and $[mn]$ to the NNN pair with a ferromagnetic (FM) exchange interaction (J^e_{FM}) on the *ab* plane,[25,26] E is the electrical field, ε_c is the dielectric susceptibility, and P_i is the electric polarization on site i in the mth CoMnO$_6$ chain.

It is believed that the interchain interactions J^e_{AFM} and J^e_{FM} are much smaller than the intrachain ones ($J^a_{\text{Mn-Co}}$, $J^a_{\text{Mn-Mn}}$, and $J^a_{\text{Co-Co}}$).[14,17] The last two ferroelectricity terms are also extremely small under a normal-measuring electric field due to the weak ferroelectric polarization; thus they can be neglected safely. These facts indicate that the system can be treated as an Ising model. As shown in Fig. 1, CCMO has a $\uparrow\uparrow\downarrow\downarrow$ spin order along the *c* axis and on the *ab* plane the spins form a triangular lattice. The $\uparrow\uparrow\downarrow\downarrow$ spin order is mainly determined by the predominant intrachain interaction, as the model can be seen as a diatomic Ising chain for ground-state polarization. However, if only the intrachain interaction is considered, the ground-state $\uparrow\uparrow\downarrow\downarrow$ spin order has two equal forms with opposite polarization [the left chain and right chain in Fig. 1(a)]. The interchain interactions on the *ab* plane, in spite of being much weaker than the intrachain ones, keep all the spin orders to be the same form. Therefore, one is allowed to argue that the intrachain interactions are mainly the origin for the short-range $\uparrow\uparrow\downarrow\downarrow$ spin order, while the interchain ones take responsibility for the long-range order of the system.

A. Elastic interaction

Different with the suggestion of Choi *et al.* in Ref. 14, we assume that the NN interaction is AFM rather than FM, which was demonstrated in Ref. 17 according to the first-principles calculation. Consulting to the exchange striction effect, for the AFM interaction between NN spin pairs, a repulsion force between the two ions with parallel spins, and an attraction force between the ones with antiparallel spins are expected. As shown in Fig. 1(a) where the dashed circles represent the original ion positions without exchange striction, the $\uparrow\uparrow\downarrow\downarrow$ spin order with alternating Mn and Co ions which breaks the inversion symmetry has two configurations (the left and right chains) inducing opposite polarizations.[14] Take the first configuration, for example [the left chain in Fig. 1(a)], all the Mn ions have an upward displacement while all the Co ions displace downward. We have the total electric polarization at the ground state ($T=0$) for the diatomic Ising spin chain with $2N$ ions,

$$
P_{\text{gs}}(T=0) = \sum_{i=1}^{2N} P_i = N(P_{\text{Mn}} + P_{\text{Co}}),
\tag{2}
$$

where N is the number of Mn-Co couples *in a unit volume*.

Here P_{Mn} and P_{Co} are the electric polarization defined with respect to the shifts of Mn and Co ions, respectively. The exchange force competing with the restoring force from the crystal lattice causes the displacement of the ions.

Along this line, an elastic Ising model is introduced to describe the exchange striction and the exchange energy terms $J_{1,i}$ and $J_{2,i}$ in Eq. (1) should contain a long-range elastic term which is too complicated to be expressed as an explicit form. We suggest a Lennard-Jones potential here for a simple tentative,[27]

$$J' = J'_0[(r_0/r_{ij})^{12} - (r_0/r_{ij})^6], \qquad (3)$$

where r_{ij} is the distance between the ions on site i and site j, and r_0 is the equilibrium distance between two interacting spins. We mark the displacement of the ion on site i as r_i, then the distance r_{ij} can be represented as $r_{ij}=r_0+r_i+r_j$. Since r_i is a relatively small quantity with respect to r_0, the elastic energy is cutoff only to the first order. The elastic interaction becomes weaker as the distance between spins grows, so only NN and NNN terms are taken into account.

Considering the elastic exchange associated with the NNN spin pair ($J_{2,i}$), no symmetry breaking is found to cause effective exchange striction, which indicates that the elastic interaction should only be applied to the NN interaction J_{Mn-Co}. Including the elastic energy from crystal lattice, we express the elastic Hamiltonian as a perturbation to Eq. (1),

$$H_1 = -J_{Mn-Co}\sum_{i,j}\frac{6(r_i+r_j)}{r_0}S_i \cdot S_j + 1/2\sum_i k_i r_i^2, \qquad (4)$$

where k_i is the stiffness factor for ion on site i.

B. Ferroelectricity at ground state

From the elastic Hamiltonian, Eq. (4), one obtains the ion equilibrium position by minimizing H_1 with respect to r_i. Therefore the displacement r_i becomes

$$r_i = -\frac{6J_{Mn-Co}S_i \cdot S_{i+1} - 6J_{Mn-Co}S_{i-1} \cdot S_i}{r_0 k_i} = \frac{-12J_{Mn-Co}S_i \cdot S_{i+1}}{r_0 k_i}. \qquad (5)$$

The electrical polarization in the ground state ($T=0$) in Eq. (2) can be expressed as

$$\begin{aligned}
P_{gs} &= N(P_{Mn} + P_{Co}) = \sum_{i=1}^{2N} Q_i \cdot r_i \\
&= N\left(Q_{Mn} \cdot \frac{-12J_{Mn-Co}S_{Mn} \cdot S_{Co}}{r_0 k_{Mn}}\right. \\
&\quad \left. -Q_{Co} \cdot \frac{-12J_{Mn-Co}S_{Mn} \cdot S_{Co}}{r_0 k_{Co}}\right), \qquad (6)
\end{aligned}$$

where Q_i is the electric charge of ion on site i (Q_{Mn}, Q_{Co}), S_{Mn} and S_{Co} are the spins of ions Mn and Co, and k_{Mn} and k_{Co} are the stiffness factors of ions Mn and Co, respectively.

For CCMO, the parallel Mn-Co chains along the c axis form a triangular lattice on the ab plane. The interchain distance between the NN chains is $a=5.24$ Å and the intrachain

distance between Mn and Co ions is $r_0=2.65$ Å.[19–21] So we obtain $N=1.57 \times 10^{28}$ m^{-3}. We also have the charges for Mn and Co ions: $Q_{Mn}=4e$ and $Q_{Co}=2e$. The spin for Mn ion is $S_{Mn}=1.305$ and for Co ion is $S_{Co}=1.24$.[17]

Furthermore, six Mn-O bonds form an octahedral prism, while six Co-O bonds form a trigonal prism. Three of the six Mn-O (or Co-O) bonds have an angle θ_{Mn} (or θ_{Co}) from the Mn-Co chain along the c axis while the others have the angle $\pi-\theta_{Mn}$ (or $\pi-\theta_{Co}$). We treat the covalent bond equivalent to a Coulomb interaction with equivalent charges $Q^*_{Mn}=\alpha_{Mn}Q_{Mn}$, $Q^*_{Co}=\alpha_{Co}Q_{Co}$, and $Q^*_O=\alpha_{Mn,Co}Q_O$ (for the O ions in Mn-O bonds and Co-O bonds, respectively) where $Q_O=2e$ is the charge of oxygen ion. Only considering the component of interaction along the c axis, the Coulomb interaction from these six bonds can be regarded as a harmonic oscillator when the displacement of the ion (Mn or Co) is small, so that the stiffness factors for these bonds can be evaluated. We have the Coulomb interaction F for the Mn-O bonds and Co-O bonds

$$\begin{aligned}
F &= \frac{3}{4\pi\varepsilon_0}\left\{\frac{Q_\mu Q_O \alpha_\mu^2 \cos(\theta_\mu)}{[R_\mu - r_\mu/\cos(\theta_\mu)]^2} + \frac{Q_\mu Q_O \alpha_\mu^2 \cos(\pi-\theta_\mu)}{[R_\mu - r_\mu/\cos(\pi-\theta_\mu)]^2}\right\} \\
&\approx \frac{3Q_\mu Q_O \alpha_\mu^2}{\pi\varepsilon_0 R_\mu^3}r_\mu, \quad \mu = Mn, Co, \qquad (7)
\end{aligned}$$

where ε_0 is the dielectric constant in vacuum, r_μ is the displacement of Mn or Co ions along the c axis, the length of Mn-O bond is $R_{Mn}=1.905$ Å, and the length of Co-O bond is $R_{Co}=2.140$ Å.[19–21] From the definition of harmonic oscillator, the stiffness factor can then be expressed as

$$k_\mu = \frac{3Q_\mu Q_O \alpha_\mu^2}{\pi\varepsilon_0 R_\mu^3}, \quad \mu = Mn, Co. \qquad (8)$$

As the bond strength for Mn-O is ~402.9 and ~384.5 kJ/mol for Co-O bond,[28,29] we obtain $k_{Mn}=221$ N/m, the stiffness factor for Mn-O bonds, and $k_{Co}=168$ N/m, the factor for Co-O bonds.

III. MEAN-FIELD THEORY AT FINITE TEMPERATURE

Given the electric polarization in the ground state, we investigate the ferroelectric and magnetic properties at nonzero T. In this section, MFT for Eq. (1) is developed to evaluate the T dependences of electricity polarization, magnetic susceptibility, and dielectric susceptibility. As discussed above, the elastic Hamiltonian is a small quantity, so the model used in the following can be simplified into a simple Ising model with the interchain interactions.

A. Order parameters and effective fields

Given the ↑↑↓↓ spin alignment with alternating Co ion and Mn ion along the c axis at the ground state, the Co ions and Mn ions on the ab plane form a triangular lattice. Viewing the atomic configuration on the ab plane, the smallest structure unit under consideration consists of four layers. Figure 1(b) depicts one layer (layer I) on the ab plane and the three layers (II, III, and IV) below it, where solid circles

represent spin up, open circles represent spin down, small circles represent Mn ions, and large circles represent Co ions [Fig. 1(b)].

For this structure unit, four order parameters should be included to construct an effective field $\sigma_\mu = \langle S_\mu \rangle$, where $\mu = 1, 2, 3,$ and 4, and $\langle S_\mu \rangle$ means the average of S_μ. Assuming that a spin chain has the configuration as shown in the left chain of Fig. 1(a), with which S_μ are marked out. In the ground state, $\mu = 1, 2, 3,$ and 4 represents Mn ions with spin up, Co ions with spin up, Mn ions with spin down, and Co ions with spin down, respectively. In the ordered phase, $\sigma_1 = S_{\text{Mn}}$, $\sigma_2 = S_{\text{Co}}$, $\sigma_3 = -S_{\text{Mn}}$, and $\sigma_4 = -S_{\text{Co}}$. Clearly, for spin-disordered phase, all the four order parameters are zero.

The mean-field theory constructed below is based on Hamiltonian Eq. (1), neglecting the last two ferroelectric terms. The effective fields from the intrachain interactions are

$$F_1^a = J_{\text{Mn-Co}}^a (\sigma_2 + \sigma_4) + 2 J_{\text{Co-Co}}^a \sigma_3$$

$$F_2^a = J_{\text{Mn-Co}}^a (\sigma_1 + \sigma_3) + 2 J_{\text{Mn-Mn}}^a \sigma_4,$$

$$F_3^a = J_{\text{Mn-Co}}^a (\sigma_2 + \sigma_4) + 2 J_{\text{Co-Co}}^a \sigma_1$$

$$F_4^a = J_{\text{Mn-Co}}^a (\sigma_1 + \sigma_3) + 2 J_{\text{Mn-Mn}}^a \sigma_2 \qquad (9)$$

where $J_{\text{Mn-Co}}^a$ is the intrachain NN spin-pair interaction, $J_{\text{Mn-Mn}}^a$ and $J_{\text{Co-Co}}^a$ are the NNN pair interactions, and F_μ^a represents the intrachain effective fields on the spin moment S_μ ($\mu = 1, 2, 3,$ and 4).

Given the spin configuration on the *ab* plane [Fig. 1(b)], we consider the interchain interaction between NN spins on the *ab* plane to be AFM and the interaction between NNN spins on the *ab* plane to be FM.[25,26] The effective fields from the interchain interactions can be expressed as

$$F_1^e = 2 J_{\text{AFM}}^e (\sigma_2 + \sigma_3 + \sigma_4) + 6 J_{\text{FM}}^e \sigma_1$$

$$F_2^e = 2 J_{\text{AFM}}^e (\sigma_1 + \sigma_3 + \sigma_4) + 6 J_{\text{FM}}^e \sigma_2,$$

$$F_3^e = 2 J_{\text{AFM}}^e (\sigma_1 + \sigma_2 + \sigma_4) + 6 J_{\text{FM}}^e \sigma_3$$

$$F_4^e = 2 J_{\text{AFM}}^e (\sigma_1 + \sigma_2 + \sigma_3) + 6 J_{\text{FM}}^e \sigma_4 \qquad (10)$$

where F_μ^e represents the interchain effective fields on the spin moment S_μ ($\mu = 1, 2, 3,$ and 4). All the AFM interactions (J_{AFM}^e) between the NN spin pairs or the FM interactions (J_{FM}^e) between the NNN spin pairs on the *ab* plane are supposed to be equal for different ions pairs. Following the standard procedure of mean-field approximation, the order parameters can be calculated from a set of self-consistent equations

$$\sigma_\mu = |S_\mu| \tanh\left(\frac{(F_\mu^a + F_\mu^e) + g_l \mu_B H}{k_B T} |S_\mu| \right), \quad \mu = 1, 2, 3, 4, \qquad (11)$$

where $|S_\mu| = S_{\text{Mn}}$ at $\mu = 1$ and 3, $|S_\mu| = S_{\text{Co}}$ at $\mu = 2$ and 4, and k_B is the Boltzmann constant. There are four degenerate solutions as $T = 0$: $\uparrow\uparrow\downarrow\downarrow$, $\downarrow\downarrow\uparrow\uparrow$, $\uparrow\downarrow\downarrow\uparrow$, and $\downarrow\uparrow\uparrow\downarrow$. Here we

find that the spin order in the ground state is the same as the one we predicted in Sec. II, and the single chain elastic Ising model (neglecting interaction between chains) is valid for the ferroelectricity in the ground state.

B. Ferroelectric polarization and spin order

With the MFT given in Eq. (11), we can derive out the dependence of polarization P on σ_μ and thus the T dependence of P. In the ground state, the $\uparrow\uparrow\downarrow\downarrow$ spin order along the c axis will be gradually broken with increasing T due to the spin excitation, thus the ferroelectricity will fall down.

First, consider a spin-flip event whose probability can be defined as $\omega_\mu = (\sigma_\mu^0 - \sigma_\mu)/(2\sigma_\mu^0)$, $\mu = 1, 2, 3,$ and 4, where σ_μ^0 is the order parameter in the ground state (ordered phase). In the mean-field framework, a direct algorithm on the configuration of one spin chain allows the following properties: (i) in the ground state, $\omega_1 = \omega_2 = \omega_3 = \omega_4 = 0$ since $\sigma_\mu = \sigma_\mu^0$ and P is given by Eq. (2); (ii) in the disordered phase, $\omega_1 = \omega_2 = \omega_3 = \omega_4 = 0.5$ since $\sigma_\mu = 0$, and $P = 0$; (iii) when parameters ω_1 and ω_3, or ω_2 and ω_4, are disordered, which means $\omega_1 = \omega_3 = 0.5$ or $\omega_2 = \omega_4 = 0.5$, P is also zero; (iv) for $\omega_1 = \omega_3 = 1$ and $\omega_2 = \omega_4 = 0$ (or $\omega_2 = \omega_4 = 1$ and $\omega_1 = \omega_3 = 0$), the spin configuration changes from the left chain of Fig. 1(a) to the right one and P becomes $-P$; (v) if all spins flip, i.e. $\sigma_\mu = -\sigma_\mu^0$, which means $\omega_1 = \omega_2 = \omega_3 = \omega_4 = 1$, the spin configuration of the chain remains the same and thus P remains unchanged.

To illustrate in a clearer manner these properties, we consider the "polarization" of a local ion, for example, a Co ion. In this case, we take care of a three-spin subsystem. Look at one Co^{2+} spin and its two NN Mn^{4+} spins. For such a subsystem, eight spin configurations are counted, which can be divided into three groups: (i) the spin alignment is $\uparrow\uparrow\downarrow$ or $\downarrow\downarrow\uparrow$, generating a polarization $P^{\text{I,II}} = P_{\text{Mn}} + P_{\text{Co}}$, as shown in Fig. 2(a); (ii) the spin alignment takes the form $\uparrow\downarrow\downarrow$ or $\downarrow\uparrow\uparrow$, resulting in a polarization $P^{\text{III,VI}} = -(P_{\text{Mn}} + P_{\text{Co}})$, opposite to $P^{\text{I,II}}$, as shown in Fig. 2(b); (iii) the spin alignment takes either FM order or AFM order: $\downarrow\downarrow\downarrow$, $\uparrow\downarrow\uparrow$, $\downarrow\downarrow\downarrow$, or $\uparrow\uparrow\uparrow$, which does not give rise to any nonzero polarization, as shown in Fig. 2(c).

Therefore, four of the eight spin configurations exhibit nonzero polarization. As an example, one configuration, with the three spins denoted as S_1, S_2, and S_3, respectively, is marked out by a coarse ellipse in Fig. 2. The ground state for this $S_1 S_2 S_3$ subsystem has a $\uparrow\uparrow\downarrow$ spin order with polarization P^{I}. In this subsystem, the probability W for the four spin configurations of nonzero P ($P^{\text{I,II,III,IV}}$) can be expressed as a function of the order parameters in the following way: (i) for the $\uparrow\uparrow\downarrow$ order, $W = W^{\text{I}} = (1 - \omega_1)(1 - \omega_2)(1 - \omega_3)$, (ii) for the $\downarrow\downarrow\uparrow$ order, one has $W = W^{\text{II}} = \omega_1 \omega_2 \omega_3$, (iii) for the $\uparrow\downarrow\downarrow$ order, $W = W^{\text{III}} = (1 - \omega_1)\omega_2(1 - \omega_3)$, and (iv) for the $\downarrow\uparrow\uparrow$ order, $W = W^{\text{VI}} = \omega_1(1 - \omega_2)\omega_3$.

The same procedure can also be applied to the other three subsystems, counted as $S_2 S_3 S_4$, $S_3 S_4 S_1$, and $S_4 S_1 S_2$. Obviously, the averaged polarization (P_{MFT}) for a 2N-spin diatomic chain is

$$P_{\text{MFT}} = N \langle P \rangle = \frac{N}{4} \sum_{\mu=1,2,3,4} (P_\mu^{\text{I}} W_\mu^{\text{I}} + P_\mu^{\text{II}} W_\mu^{\text{II}} + P_\mu^{\text{III}} W_\mu^{\text{III}}$$

$$+ P_\mu^{\text{VI}} W_\mu^{\text{VI}}) = N(P_{\text{Mn}} + P_{\text{Co}})[1 - (\omega_1 + \omega_2 + \omega_3 + \omega_4)$$

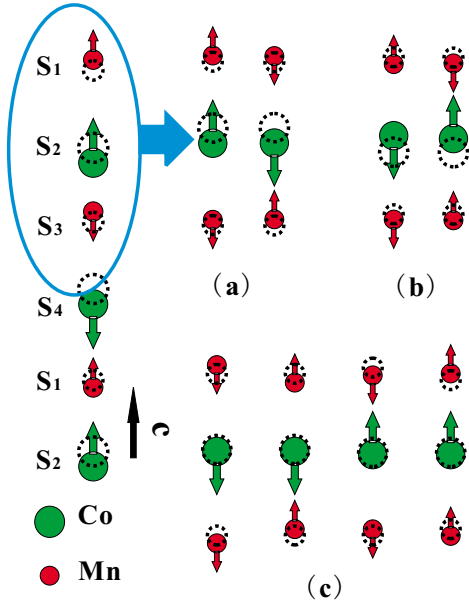$$+ (\omega_1 + \omega_3)(\omega_2 + \omega_4)], \qquad (12)$$

FIG. 2. (Color online) Eight spin configurations for the three spins (S_1, S_2, and S_3). They are classified into three groups with different polarizations: (a) $P=P_{Mn}+P_{Co}$, (b) $P=-(P_{Mn}+P_{Co})$, (c) $P=0$.

which is the main result of the MFT, dealing with the T dependence of polarization P. It is found that Eq. (12) fully meets the condition defined above for the relationship between P and σ_μ ($\mu=1$, 2, 3, and 4). For instance, in the ground state, $\omega_1=\omega_2=\omega_3=\omega_4=0$, then $P_{MFT}=N(P_{Mn}+P_{Co})$, same as Eq. (2).

C. Polarization domains

As in the discussion before, the interchain interactions keep the polarization direction of the CoMnO₆ chains coherent, but such a long-range order is not stable at finite temperature since the interchain interactions are much weaker than the intrachain ones. It is known that MFT cannot work well on the system while long-range order is broken, and then a correction to this deficiency should be added to our model. Therefore, the formation of polarization domains is preferred. In fact similar consideration of the polarization domains was suggested earlier.[17] This effect may not influence significantly the transition temperature for ferroelectricity but play an important role in modulating the magnitude of polarization. The rationality of this correction will be proven below by the quantitative consistency of the model calculation with experimental data.

Furthermore, from Eq. (11) it is easily inferred that the ground state at $T=0$ has four spin alignments which are degenerate in energy: $\uparrow\uparrow\downarrow\downarrow$, $\downarrow\downarrow\uparrow\uparrow$, $\uparrow\downarrow\downarrow\uparrow$, and $\downarrow\uparrow\uparrow\downarrow$. The former two ($\uparrow\uparrow\downarrow\downarrow$ and $\downarrow\downarrow\uparrow\uparrow$), shown as the left chain in Fig. 1(a), have an upward polarization while the latter two ($\uparrow\downarrow\downarrow\uparrow$ and $\downarrow\uparrow\uparrow\downarrow$) have a downward polarization, shown as the right chain in Fig. 1(a). It is easy to conclude that the reversal of a polarization domain should meet the condition: either $\sigma_{1,3}\rightarrow-\sigma_{1,3}$ while $\sigma_{2,4}$ remains invariable or $\sigma_{2,4}\rightarrow-\sigma_{2,4}$ while $\sigma_{1,3}$ remains invariable. Because of these degen-
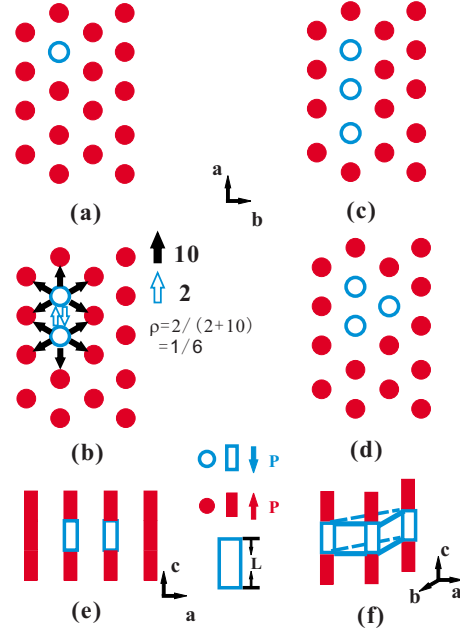

FIG. 3. (Color online) [(a)–(d)] Four exampled polarization domains viewed on the *ab* plane. In (b) the bonds on the domain wall and bonds inside the domain are shown, by which parameter ρ is calculated. (a) $\rho=0$, (b) $\rho=1/6$, (c) $\rho=2/9$, and (d) $\rho=1/3$. (e) shows the *ac*-plane projection of the domain shown in (b). (f) shows the three-dimensional pattern of the domain shown in (d).

erate spin-order states, the existence of polarization domains at a nonzero T is a reasonable argument. Therefore, we need to take into account the polarization domain-wall energy. We focus on the domains with downward polarization and evaluate the energy for them to reverse from the upward polarization matrix. Two terms have contribution to the excited energy: one is the change in the interchain interactions and the other is the Zeeman energy from magnetic field.

Clearly, the smallest polarization unit is a CoMnO₆ chain of four spins along the c axis, either taking the form $\uparrow\uparrow\downarrow\downarrow/\downarrow\downarrow\uparrow\uparrow$ or $\uparrow\downarrow\downarrow\uparrow/\downarrow\uparrow\uparrow\downarrow$ at the ground state. To characterize any polarization domain consisting of one or more such units, we need three parameters. First, we denote by parameter L the number of the units along the c axis (i.e., domain height). Second, parameter $\rho\in[0,1]$ is the clustering degree of the domains on the *ab* plane. Third, parameter η describes the total change in spin moment for the reversal of this domain. It is easy to see that the excited energy is proportional to L which is supposed to be a constant given field h.

The clustering degree ρ is supposed to measure the effect of the interchain interactions and it scales roughly the domain size on the *ab* plane. In Fig. 3 several simple polarization domains on the *ab* plane are shown (each circle on the *ab* plane represents a polarization unit), which are, respectively, embedded in the matrix of the opposite domain. In Fig. 3(b) an example to evaluate parameter ρ is given, and we only consider the effect from the NN interchain interaction. We define $\rho=2/12=1/6$. Similarly, one has $\rho=0$ for the domain in Fig. 3(a), $\rho=2/9$ for the domain in Fig. 3(c), and $\rho=1/3$ for the domain in Fig. 3(d). With such a definition,

we see that the excited energy associated with reversal of a new domain from the parent domain is proportional to $(1 - \rho)$ normalized by the number of the in-plane polarization units inside this new domain.

For parameter η, the change in spin moment is from 0 to $2g_l\mu_B(\sigma_1 + \sigma_3)$ for domains of up polarization and from 0 to $2g_l\mu_B(\sigma_2 + \sigma_4)$ for domains of down polarization. So η changes between 0 and 2 upon any domain reversal.

Consequently, the excited energy for reversal of the two types of domains (up and down polarization) can be expressed as

$$\Delta E_1 = L(1-\rho)2(F_1^e\sigma_1 + F_3^e\sigma_3) + Lh\eta g_l\mu_B(\sigma_1 + \sigma_3),$$

$$\Delta E_2 = L(1-\rho)2(F_2^e\sigma_2 + F_4^e\sigma_4) + Lh\eta g_l\mu_B(\sigma_2 + \sigma_4),$$

$$(13)$$

where η is a constant for a specific domain. Following the Boltzmann excitation, the probability for reversal of the two types of domains are

$$W_{d1} = \exp\left(\frac{-\Delta E_1}{k_B T}\right) \Big/ \left[1 + \exp\left(\frac{-\Delta E_1}{k_B T}\right)\right]$$

$$W_{d2} = \exp\left(\frac{-\Delta E_2}{k_B T}\right) \Big/ \left[1 + \exp\left(\frac{-\Delta E_2}{k_B T}\right)\right]. \quad (14)$$

D. Polarization, magnetic susceptibility, and dielectric susceptibility

We consider the probability for domain reversal over the whole lattice as the average of W_{d1} and W_{d2} in Eq. (14), i.e., $W_{\text{domain}} = (W_{d1} + W_{d2})/2$. The final polarization given by the MFT plus polarization domain correction (denoted by MFT +DC) is $P_{\text{MFT+DC}}$,

$$P_{\text{MFT+DC}} = P_{\text{MFT}} \cdot (1 - 2 \cdot W_{\text{domain}}). \quad (15)$$

When H is very small, the magnetic susceptibility can be defined as

$$\chi_{\text{MFT}} = M/h = g_l\mu_B(\sigma_1 + \sigma_2 + \sigma_3 + \sigma_4)/h. \quad (16a)$$

With the polarization domain correction, the magnetic susceptibility is

$$\chi_{\text{MFT+DC}} = \chi_{\text{MFT}} \cdot (1 - \eta \cdot W_{\text{domain}}). \quad (16b)$$

Similar to the calculation of $\langle P \rangle$ in Eq. (12), the average of P^2 is

$$\langle P^2 \rangle = \frac{1}{4}\sum_{\mu=1,2,3,4}[(P_\mu^{\text{I}})^2 W_\mu^{\text{I}} + (P_\mu^{\text{II}})^2 W_\mu^{\text{II}} + (P_\mu^{\text{III}})^2 W_\mu^{\text{III}}$$

$$+ (P_\mu^{\text{VI}})^2 W_\mu^{\text{VI}}] = (P_{\text{Mn}} + P_{\text{Co}})[1 - 0.5(\omega_1 + \omega_2 + \omega_3 + \omega_4) + \omega_1\omega_3 + \omega_2\omega_4]. \quad (17)$$

Noting that the reversal of polarization domains, which makes P into $-P$, does not change the value of $\langle P^2 \rangle$, the dielectric susceptibility can be calculated from statistic fluctuation[24]

TABLE I. Parameters chosen in the model calculations.

$J_{\text{Mn-Co}}^a$ (meV)	-0.5	S_{Mn} (μ_B)	1.305
$J_{\text{Co-Co}}^a$ (meV)	-0.55	S_{Co} (μ_B)	1.24
$J_{\text{Mn-Mn}}^a$ (meV)	-0.45	L ($h=0, 4, 7$ T)	12, 8, 5
J_{AFM}^e (μeV)	-2	ρ ($h=0, 4, 7$ T)	0.7, 0.6, 0.55
J_{FM}^e (μeV)	2	η	0.4
g_L	2	ε' (relative unit)	40

$$\varepsilon_c = \varepsilon' + \frac{(\langle P^2 \rangle - \langle P \rangle^2)}{T}, \quad (18)$$

where ε' is the dielectric susceptibility contributed from other ions in CCMO system, and it is suggested to be a constant.

IV. RESULTS AND DISCUSSION

A. Comparison with experiment

In this section, we present our model calculation on the T-dependent polarization, magnetic susceptibility, and dielectric susceptibility, and compare them with the measured data taken from Ref. 14. The parameters chosen for our calculation are shown in Table I.

By taking $J_{\text{Mn-Co}} = -0.5$ meV into Eq. (6), one obtains the electric polarization in the ground state $P_{\text{gs}} \sim 92$ $\mu\text{C/m}^2$. With the assumption of no structure changes while x is very close to 1.0 ($x < 1$), we treat the $\text{Ca}_3\text{Co}_{2-x}\text{Mn}_x\text{O}_6$ as $(x)\text{Ca}_3\text{CoMnO}_6 \bullet (1-x)\text{Ca}_3\text{Co}_2\text{O}_6$ for simplicity. It is rough but still reasonable since the Co prefers to occupy the trigonal prism site while the Mn prefers the octahedron site due to the chemical stability, as aforementioned. Therefore, when there's a tiny non-stoichiometry-like $x = 0.04$, the main up-up-down-down spin structures and Co-Mn alternation should be kept although there are some $\text{Ca}_3\text{Co}_2\text{O}_6$ insertions. Since it is known that no electrical polarization in $\text{Ca}_3\text{Co}_2\text{O}_6$ system is available, the ground-state polarization can be expressed as a viable to x, $P = N(P_{\text{Mn}} + P_{\text{Co}})x$. For $x = 0.96$, we obtain $P \sim 88$ $\mu\text{C/m}^2$, and this value is very close to the measured data $P \sim 90$ $\mu\text{C/m}^2$ at $T = 2$ K.[14] Of course, to fully account this nonstoichiometry issue, the correlation between the excessive Co should be considered, which is very complex (especially when x is large) and certainly beyond the current work.

Figures 4(a)–4(c) present the calculated polarization P (open circle dots: MFT; open square dots: MFT+DC), as a function of T under several fields h. The measured data taken from Ref. 14 are also plotted in the figures (solid circle dots: experiment) for comparison. It is clearly shown that the temperature dependence of P from the MFT has agreeable T_c (about 16 K) of ferroelectricity with experiment data, and the polarization from the MFT+DC shows quite good agreement with the measured one. This perfect agreement suggests that the present mean-field theory captures the essence of ferroelectricity generation in CCMO.

Figures 5(a) and 5(b) present the calculated magnetic and dielectric susceptibilities (χ and ε) as a function of T for a
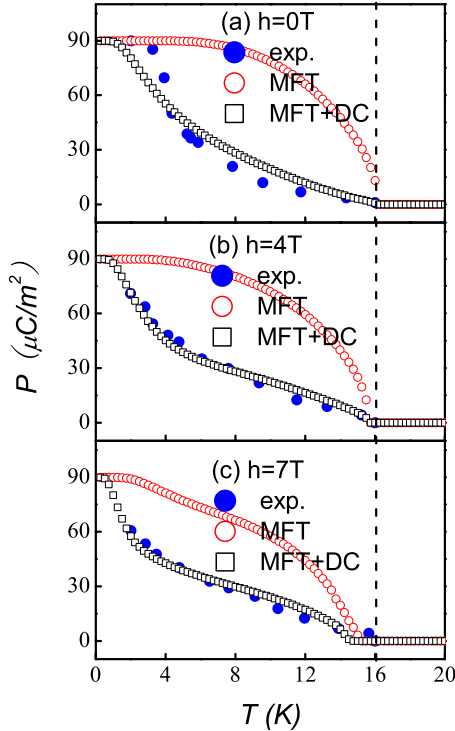
FIG. 4. (Color online) Electric polarization P as a function of T, calculated from the MFT (open circle), MFT+DC (open square), and taken from experiment (full circle, Ref. 14). (a) $h=0$ T, (b) h =4 T, and (c) $h=7$ T.
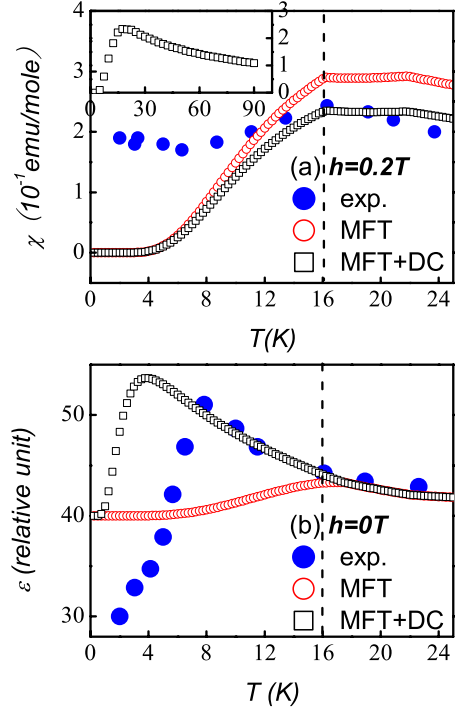

FIG. 5. (Color online) (a) Magnetic susceptibility χ and (b) dielectric susceptibility ε as a function of T, calculated by the MFT (open circle), MFT+DC (open square), and taken from experiment (full circle, Ref. 14). The inset in (b) shows χ from $T=0 \sim 90$ K.

comparison with experimental data. It is seen that the calculated χ under $h=0.2$ T and ε under $h=0$ are on the same order of magnitude with measured data. For details, the measured $\chi(T)$ has a nonzero value at $T=0$ K, while the calculated one is zero for the AFM interaction between the NN spin pairs both along the c axis and on the ab plane. At low T (about $2 \sim 5$ K) the measured $\chi(T)$ has a U-type-like behavior, while the calculated one increases monotonously. However both the two $\chi(T)$ curves have the same Neel point. We shall discuss the possible reason for the difference. It should be addressed that the calculated $\varepsilon(T)$ shows similar behavior to the measured one, and they both exhibit the single peak pattern against temperature.

B. Discussion

Our model focuses on an Ising model with diatomic chains along the c axis and triangular lattice on the ab plane. Real CCMO samples are much more complicated. We address the rationality of our MFT theory and also the reason for the difference between experiment data and our MFT calculation.

Parameters in Table I are chosen to fit the experiment data and are also validated by the rationality of the choice if one consults to earlier works.[14–24] However, these earlier works gave quite scattered results and a careful choice of the parameters is based on our discussion presented below.

First, according to the first-principles calculation,[17] the NN intrachain interaction (J_{Mn-Co}) is AFM rather than FM,

which is inconsistent with the suggestion by Choi *et al.*[14] However, the bonds between parallel Mn and Co spins are still shortened even with the AFM interaction between the NN spin pairs in Ref. 17, and the displacements are attributed to the direct metal-metal bonding, which is stronger between ions with identical spin than the one with opposite spins.[17,30] Since the calculated polarization in Ref. 17 is unreasonably large (about 200 times larger than the experimental one), we question the reliability of this calculation. We still believe that it is the exchange striction to take responsibility for the ferroelectricity in CCMO system in this paper. In Table I, J_{Mn-Co} is chosen favoring the AFM order, as the calculation with the FM interaction does not agree with experiment data. With a FM interaction between the NN spin pairs, a high h (=4 and 7 T) may induce a FM order rather than a $\uparrow\uparrow\downarrow\downarrow$ order. This is also a disadvantage for the assumption of a FM interaction between the NN spin pairs.

Second, it is also found that the chosen exchange interactions (J_{Mn-Co}, J_{Mn-Mn}, and J_{Co-Co}) in Table I (-0.5, -0.55, and -0.45 meV) are much smaller than those taken for first-principles calculation in Ref. 17 (-3.34, -2.09, and -1.63 meV). We present our calculated order parameters as functions of T in Fig. 6(a). It is seen that the calculated behaviors are quite well consistent with experimental observations given in Ref. 14, in several ways below: (i) experiment finds no significant change in magnetic structure at $T=8$ K from the ground state, while the calculated order parameters in Fig. 6(a) remain invariable from $T=0$ to $T=8$ K. (ii) Experimentally, ferroelectricity appears below $T \sim 16$ K while order parameters σ_2 and σ_4 become fully disordered at $T=16$ K. (iii) Experimentally, no magnetic or-
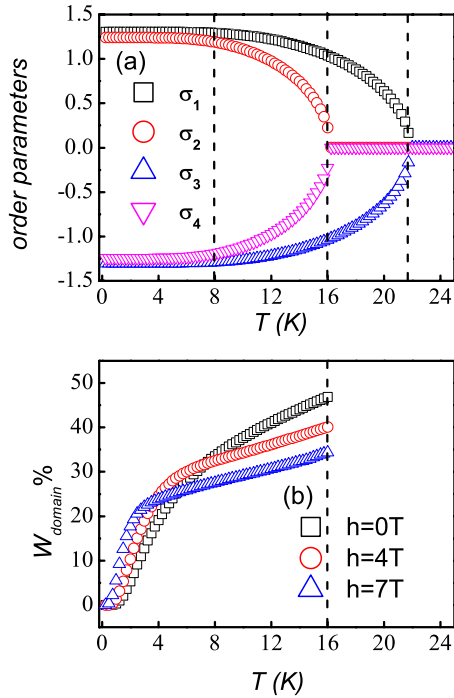
FIG. 6. (Color online) (a) Four order parameters as a function of T at $h=0$, and (b) probability W_{domain} for polarization domain reversal as a function of T under various magnetic field h (=0, 4, and 7 T).

der above $T=20$ K was observed, while all the order parameters are zero at $T>21$ K. These good consistencies indicate that the exchange interactions we choose are more suitable than the predicted values in Ref. 17.

Third, for parameters L and ρ, we find that magnetic field h reduces the dimension of the domains along the c axis and the clustering degree on the ab plane. The mean thickness of the domain along the c axis is reduced from about 127.2 Å ($h=0$ T) to 53 Å ($h=7$ T). As we see, the assumption we made for polarization domains is simple but reasonable for CCMO.

Fourth, we find that external magnetic field h suppresses the ferroelectricity at low T (<6 K) but enhances it at high T (>6 K), which was rarely observed in other multiferroics but it is true for CCMO. The weak interchain interactions, compared with the intrachain interactions, are suggested to be the microscopic mechanism for the polarization domain reversal at high T, which inversely breaks the long-range spin order along the c axis. It is tentative for us to attribute the response of polarization against h to the breaking of the long-range spin order. Our calculation, as shown in Fig. 6(b),

indicates that the probability for polarization domain reversal with increasing h is reduced at $T>6$ K, while it is enhanced at $T<6$ K. This means that magnetic field h stabilizes the long-range spin order at $T>6$ K and destabilizes the order below 6K, noting that h always unfavors the short-range AFM spin order for all temperatures. It is concluded that the competition between the short-range order and long-range order under magnetic field causes the different h dependences of polarization at low T and high T.

Fifth, what should be mentioned and also shown in Fig. 5(a) is that the calculated $\chi(T)$ does not coincide with experiment data in the low-T range. In fact, the clean end compound of CCMO, i.e., CCO, was investigated carefully as a triangular Ising model system,[25,26,31] and the model predictions have similar difference with observed magnetic susceptibility in the low-T range. It is suggested that the magnetic property of CCMO can not be simply explained by the Ising spin of Mn and Co ions alone and the low-T quantum fluctuations seems to be important.

Finally, we look at the dielectric susceptibility shown in Fig. 5(b). The calculated and measured data have similar T tendency and good consistency between them in the high-T range is identified. The difference in the low-T range remains unclear to us and may be caused by the deficiency of the MFT.

V. CONCLUSION

In summary, we have proposed an elastic Ising model which has been demonstrated to predict properly the ferroelectricity generation in Ca_3CoMnO_6 as a multiferroic system with collinear spin order. A mean-field theory to this model has also been developed. With the consideration of the dynamics of polarization domains, we have improved the consistency between the MFT calculation and measured result in dielectric and ferroelectric properties. The $\uparrow\uparrow\downarrow\downarrow$ magnetic order with alternating Co and Mn ions and the elastic exchange energy are considered to be responsible for the ion displacements and, thus, the ferroelectricity. The competition between the stability of the short-range and short-order spin orders is suggested to have impact on polarization, but only the stability of the short-range spin order determines the ferroelectric transition.

*Corresponding author: liujm@nju.edu.cn

[1] D. I. Khomskii, J. Magn. Magn. Mater. **306**, 1 (2006).

[2] Y. Tokura, Science **312**, 1481 (2006).

[3] S. W. Cheong and M. Mostovoy, Nature Mater. **6**, 13 (2007).

[4] M. Fiebig, J. Phys. D **38**, R123 (2005).

[5] H. Katsura, N. Nagaosa, and A. V. Balatsky, Phys. Rev. Lett. **95**, 057205 (2005).

[6] C. Jia, S. Onoda, N. Nagaosa, and J. H. Han, Phys. Rev. B **76**, 144424 (2007).

[7] I. A. Sergienko and E. Dagotto, Phys. Rev. B **73**, 094434 (2006).

[8] I. A. Sergienko, C. Şen, and E. Dagotto, Phys. Rev. Lett. **97**, 227204 (2006).

[9] Q. C. Li, S. Dong, and J.-M. Liu, Phys. Rev. B **77**, 054442 (2008).

[10] I. Dzyaloshinskii, Sov. Phys. JETP **19**, 960 (1964).

[11] T. Moriya, Phys. Rev. **120**, 91 (1960).

[12] J. P. Hu, Phys. Rev. Lett. **100**, 077202 (2008).

[13] L. C. Chapon, P. G. Radaelli, G. R. Blake, S. Park, and S.-W. Cheong, Phys. Rev. Lett. **96**, 097601 (2006).

[14] Y. J. Choi, H. T. Yi, S. Lee, Q. Huang, V. Kiryukhin, and S.-W. Cheong, Phys. Rev. Lett. **100**, 047601 (2008).

[15] Y. J. Jo, S. Lee, E. S. Choi, H. T. Yi, W. Ratcliff, Y. J. Choi, V. Kiryukhin, S. W. Cheong, and L. Balicas, Phys. Rev. B **79**, 012407 (2009).

[16] H. Wu, T. Burnus, Z. Hu, C. Martin, A. Maignan, J. C. Cezar, A. Tanaka, N. B. Brookes, D. I. Khomskii, and L. H. Tjeng, Phys. Rev. Lett. **102**, 026404 (2009).

[17] Y. Zhang, H. J. Xiang, and M.-H. Whangbo, Phys. Rev. B **79**, 054432 (2009).

[18] M. E. Fisher and W. Selke, Phys. Rev. Lett. **44**, 1502 (1980).

[19] S. Rayaprol, K. Sengupta, and E. V. Sampathkumaran, Solid State Commun. **128**, 79 (2003).

[20] H. Wu, M. W. Haverkort, Z. Hu, D. I. Khomskii, and L. H. Tjeng, Phys. Rev. Lett. **95**, 186401 (2005).

[21] V. G. Zubkov, G. V. Bazuev, A. P. Tyutyunnik, and I. F. Berger, J. Solid State Chem. **160**, 293 (2001).

[22] H. Kageyama, K. Yoshimura, K. Kosuge, M. Azuma, M. Takano, H. Mitamura, and T. Goto, J. Phys. Soc. Jpn. **66**, 3996 (1997).

[23] Y. B. Kudasov, Phys. Rev. Lett. **96**, 027212 (2006).

[24] X. Y. Yao and V. C. Lo, J. Appl. Phys. **104**, 083919 (2008).

[25] X. Y. Yao, S. Dong, and J.-M. Liu, Phys. Rev. B **73**, 212415 (2006).

[26] X. Y. Yao, S. Dong, H. Yu, and J.-M. Liu, Phys. Rev. B **74**, 134421 (2006).

[27] X. Zhu, D. P. Landau, and N. S. Branco, Phys. Rev. B **73**, 064115 (2006).

[28] J. B. Pedley and E. M. Marshall, J. Phys. Chem. Ref. Data **12**, 967 (1984).

[29] David R. Lide, *CRC Handbook of Chemistry and Physics*, (CRC, Boca Raton, 2003–2004).

[30] D. Dai, H. J. Xiang, and M.-H. Whangbo, J. Comput. Chem. **29**, 2187 (2008).

[31] V. Hardy, S. Lambert, M. R. Lees, and D. McK. Paul, Phys. Rev. B **68**, 014424 (2003).